Electronic Supplementary Material (ESI) for RSC Advances.

A novel fluorescent pH probe with valuable pK_a based on twisted intramolecular charge transfer mechanism, and its applications in cell imaging

Fang Yu,[a, ‡] Yan Wang,[b, ‡] Wencheng Zhu,[c] Yan Huang,[a] Minghui Yang, [b, *] Hua Ai[c,*] and Zhiyun Lu[a,*]

[a]Key Laboratory of Green Chemistry and Technology of Ministry of Education, College of Chemistry, Sichuan University, Chengdu, 610064, PR China
[b]Key Laboratory of Magnetic Resonance in Biological Systems, State Key Laboratory of Magnetic Resonance and Atomic and Molecular Physics, Wuhan Centre for Magnetic Resonance, Wuhan Institute of Physics and Mathematics, Chinese Academy of Sciences, Wuhan, 430071, PR China
[c]National Engineering Research Center for Biomaterials, Sichuan University, Chengdu, 610064, PR China

Contents

1 Single-crystal X-ray crystallography and photophysical characteriazation data of the four compounds

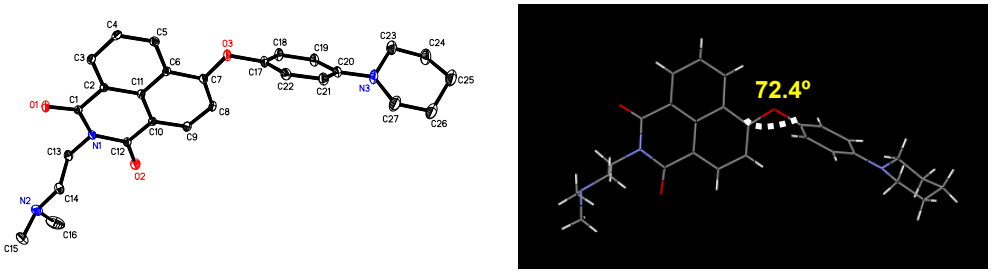

Figure S1 ORTEP drawing (hydrogen atoms removed for clarity, ellipsoids at 30% probability) and crystal structure of **Napa-pp**.

Table S1 Crystal Data and Structure Refinement for Compound **Napa-pp**

Compound	**Napa-pp**
Empirical formula	$C_{27}H_{29}N_3O_3$
Formula weight	443.53
Temperature	140.00(10) K
Crystal system	Triclinic
Space group	*P*-1
a	6.6657(12) Å
b	8.9418(16) Å
c	19.201(4) Å
α	87.395(3) deg
β	87.173(4) deg
γ	88.605(4) deg
Volume	1141.6(4) $Å^3$
Z	2
Calculated density	1.2903(5) g cm^{-3}
Absorption coefficient	0.085
F(000)	472.0
Crystal size	0.04 × 0.15 × 0.30 mm
Reflections collected	11107
Independent reflections	6601[R(int) = 0.0373]
θ-range For data collection	1.06 to 30°
Goodness-of-fit on F ^ 2	1.071
Final *R* indices[I>2σ(I)]	R_1 = 0.0703, wR_2 = 0.1944
Largest diff. peak and hole	0.64 and -0.34 e $Å^{-3}$

Table S2 Photophysical Data of **Nap-p**, **Napa-p**, **Nap-pp** and **Napa-pp** in Solvents with Different Polarities

Solvent	**Nap-p**			**Napa-p**			**Nap-pp**			**Napa-pp**		
	λ_{abs} (nm)	λ_{em} (nm)	PLQY	λ_{abs} (nm)	λ_{em} (nm)	PLQY	λ_{abs} (nm)	λ_{em} (nm)	PLQY	λ_{abs} (nm)	λ_{em} (nm)	PLQY
Tol	357	419	0.86	357	422	-	363	413	0.004	363	412	0.001
$CHCl_3$	361	426	0.81	364	438	0.486	367	418	0.003	368	423	0.003
CH_2Cl_2	359	427	0.81	362	439	0.230	360	424	0.004	367	415	0.004
MeCN	356	432	0.33	358	441	0.023	363	440	0.001	366	441	0.001
DMSO	360	443	0.087	360	444	0.007	365	442	0.003	364	442	0.003

Tol denotes toluene; MeCN denotes acetonitrile; DMSO denotes dimethylsulfoxide.

PLQYs were determined using quinoline sulfate as reference (λ_{ex} = 365 nm, λ_{em} = 415 nm).

The PLQY of **Napa-p** in Tol could not be determined exactly due to its poor solubility.

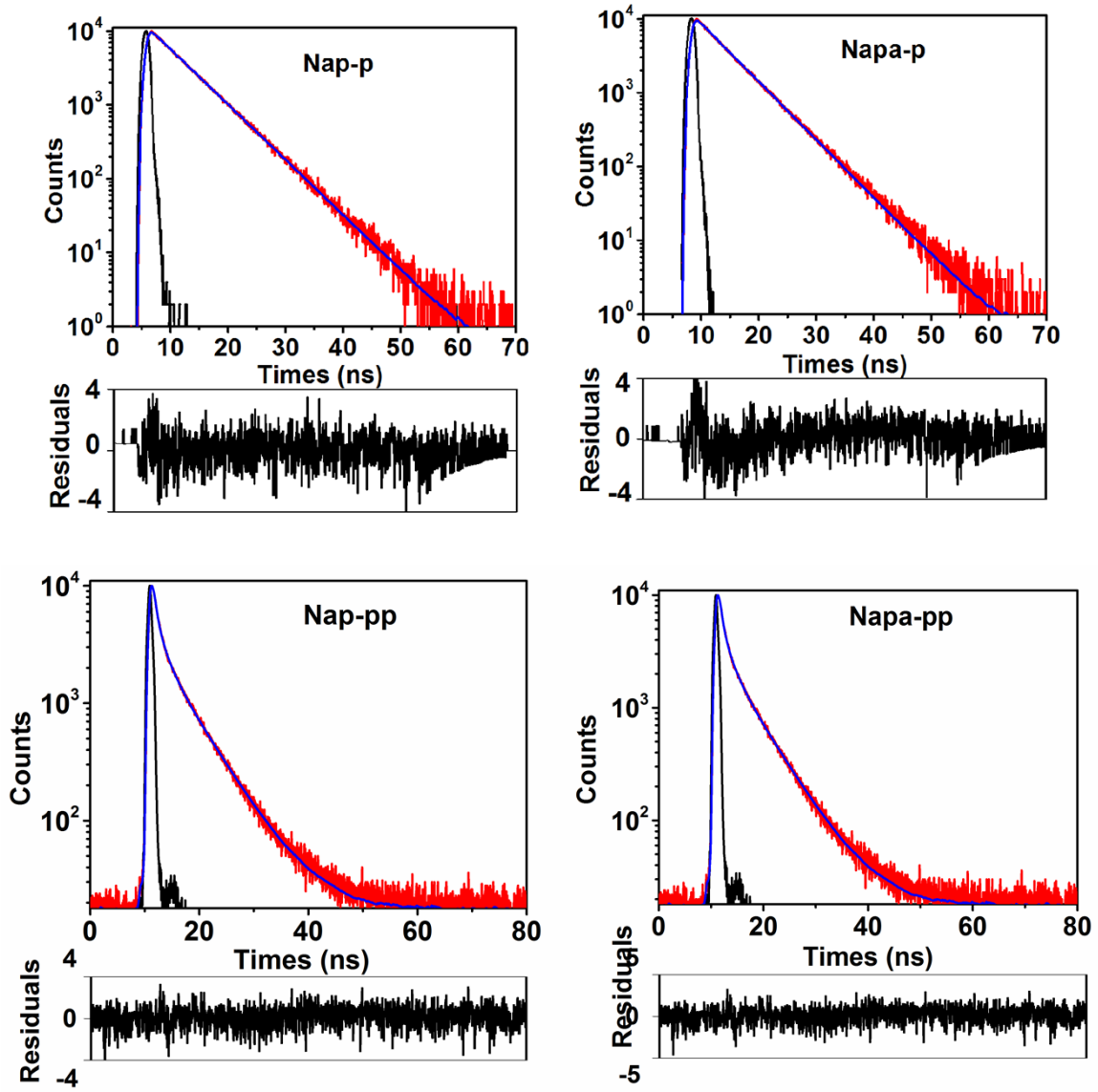

Figure S2 Fluorescence decay curves of **Nap-p**, **Napa-p**, **Nap-pp** and **Napa-pp** (1 μM in chloroform).

Table S3 Comparison of Calculated Geometry for **Napa-pp** with Experimental Data from X-ray Crystallography Analysis

Bond Lengths (Å)			Bond Angles (deg)			Dihedral Angles (deg)		
	Exp.[a]	Cal.[b]		Exp.[a]	Cal.[b]		Exp.[a]	Cal.[b]
O(1)-C(1)	1.220	1.229	O(1)-C(1)-N(1)	120.3	120.4	C(12)-N(1)-C(1)-O(1)	-175.5	-177.7
O(2)-C(12)	1.223	1.229	O(1)-C(1)-C(2)	122.7	122.8	C(13)-N(1)-C(1)-O(1)	1.1	0.9
O(3)-C(7)	1.375	1.361	O(2)-C(12)-N(1)	119.7	120.2	O(1)-C(1)-C(2)-C(3)	-3.8	-0.9
O(3)-C(17)	1.404	1.401	O(2)-C(12)-C(10)	123.2	123.1	N(1)-C(1)-C(2)-C(3)	177.0	178.9
O(3)-C(17)	1.404	1.401	O(3)-C(7)-C(6)	113.7	115.1	C(17)-O(3)-C(7)-C(8)	-4.5	6.5
N(1)-C(1)	1.394	1.402	C(7)-O(3)-C(17)	118.7	120.3	C(27)-N(3)-C(20)-C(19)	-152.2	-169.5
N(1)-C(12)	1.402	1.408	C(1)-N(1)-C(12)	125.0	125.0	C(5)-C(6)-C(7)-O(3)	0.4	0.4
N(1)-C(13)	1.469	1.473	C(1)-N(1)-C(13)	118.4	117.4	C(7)-O(3)-C(17)-C(22)	-106.5	-105.0
N(2)-C(16)	1.440	1.461	C(12)-N(1)-C(13)	116.6	117.6	C(7)-O(3)-C(17)-C(18)	76.6	79.4
N(2)-C(15)	1.453	1.460	C(16)-N(2)-C(15)	110.4	110.5	C(22)-C(17)-C(18)-C(19)	1.1	0.7
N(2)-C(14)	1.456	1.463	C(16)-N(2)-C(14)	110.9	112.5	O(3)-C(17)-C(18)-C(19)	177.9	176.2
N(3)-C(23)	1.414	1.475	C(15)-N(2)-C(14)	109.4	111.2	C(1)-N(1)-C(13)-C(14)	-90.6	-86.2
N(3)-C(20)	1.413	1.408	C(23)-N(3)-C(20)	116.9	117.0	C(12)-N(1)-C(13)-C(14)	86.2	92.4
N(3)-C(27)	1.441	1.465	C(23)-N(3)-C(27)	118.9	112.5	C(16)-N(2)-C(14)-C(13)	70.8	74.9
			C(20)-N(3)-C(27)	118.7	117.9	C(15)-N(2)-C(14)-C(13)	-167.2	-160.6
			C(1)-N(1)-C(12)	125.0	124.0	C(23)-N(3)-C(20)-C(19)	54.3	51.3

[a] Values derived from X-ray Crystallography data. [b] Values calculated at DFT//B3LYP/6-31G (d) Level with Gaussian 09.

Note: The close similarity between calculated and experimental values reveals the reliability of our computational results.

Table S4 Selected Electronic Excitation Energies (eV) and Corresponding Oscillator Strengths (*f*), Main Configurations and CI Coefficients for **Napa-pp** And Double Protonated **Napa-pp** [**Napa-pp + 2H$^+$**]. Calculated by TDDFT//B3LYP/6-31G (d), Based on the DFT//B3LYP/6-31G (d) Optimized Ground State Geometries.

	electronic transition	energy (eV) [b]	*f* [c]	Composition [d]	CI [e]
Napa-pp	$S_0 \rightarrow S_1$	2.73 (455nm)	0.0163	H→L	0.7054
	$S_0 \rightarrow S_2$	3.06 (405nm)	0.0009	H-1→L	0.7062
	$S_0 \rightarrow S_3$	3.43 (362nm)	0.3825	H-2→L	0.6967
Napa-pp + 2H$^+$	$S_0 \rightarrow S_1$	3.45 (359nm)	0.3981	H→L	0.6978
	$S_0 \rightarrow S_2$	3.97 (312nm)	0.0002	H-2→L	0.6739
	$S_0 \rightarrow S_3$	4.08 (304nm)	0.0199	H-1→L	0.6239
				H→L+4	0.2244

[a] Only selected excited states were considered. The numbers in parentheses are the excitation energy in wavelength.

[b] Oscillator strength.

[c] H stands for HOMO and L stands for LUMO. Only the main configurations are presented (CI coefficients > 0.2).

[d] CI coefficients are in absolute values.

Note: For **Napa-pp**, the excitation with the largest oscillator strength is the transition from S_0 to S_3 states. The calculated excitation energy for this transition is 362 nm, which is in good agreement with the UV-Vis absorption maximum at 367 nm, validating the reliability of our theoretical calculation results.

Table S5 Main Optimized Bong Lengths, Bond Angles and Dihedral Angles of **Napa-pp** and Double Protonated **Napa-pp** (**Napa-pp + 2H$^+$**) in Ground State and The First Excited State at DFT//B3LYP/6-31G (d) and TD-DFT//B3LYP/6-31G (d) Level with Gaussian 09 (for The Numbering of the Corresponding Atoms, See Figure S2).

		Ground State		The First Excited State	
		Napa-pp	**Napa-pp + 2H$^+$**	**Napa-pp**	**Napa-pp + 2H$^+$**
Bond Lengths	O(3)-C(7)	1.361 Å	1.368 Å	1.422 Å	1.358 Å
	O(3)-C(17)	1.401 Å	1.387 Å	1.335 Å	1.373 Å
Bond Angles	C(7)-O(3)-C(17)	120.3 deg	120.7 deg	120.1 deg	123.4 deg
Dihedral Angle	C(7)-O(3)-C(17)-C(18)	79.4 deg	75.7 deg	-1.5 deg	37.4 deg
	C(17)-O(3)-C(7)-C(8)	6.5 deg	9.8 deg	95.1 deg	31.2 deg

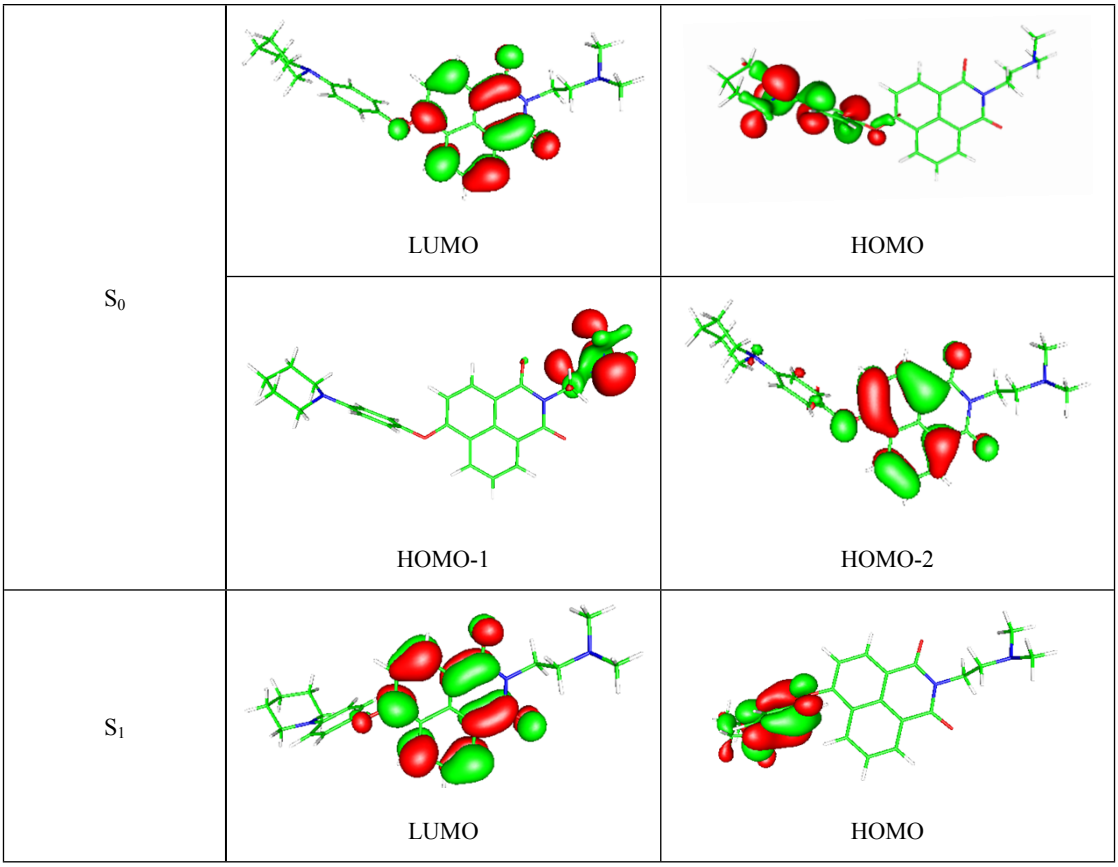

Figure S3 The calculated frontier molecular orbitals (MO) of **Napa-pp** in the ground state (S_0) and the first excited state (S_1).

S_0	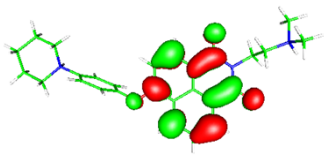 LUMO	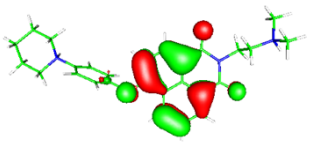 HOMO
S_1	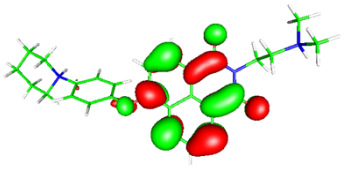 LUMO	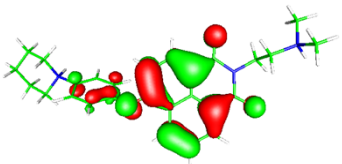 HOMO

Figure S4 The calculated frontier molecular orbitals (MO) of double protonated **Napa-pp** (**Napa-pp + 2H**$^+$) in the ground state (S_0) and the first excited state (S_1).

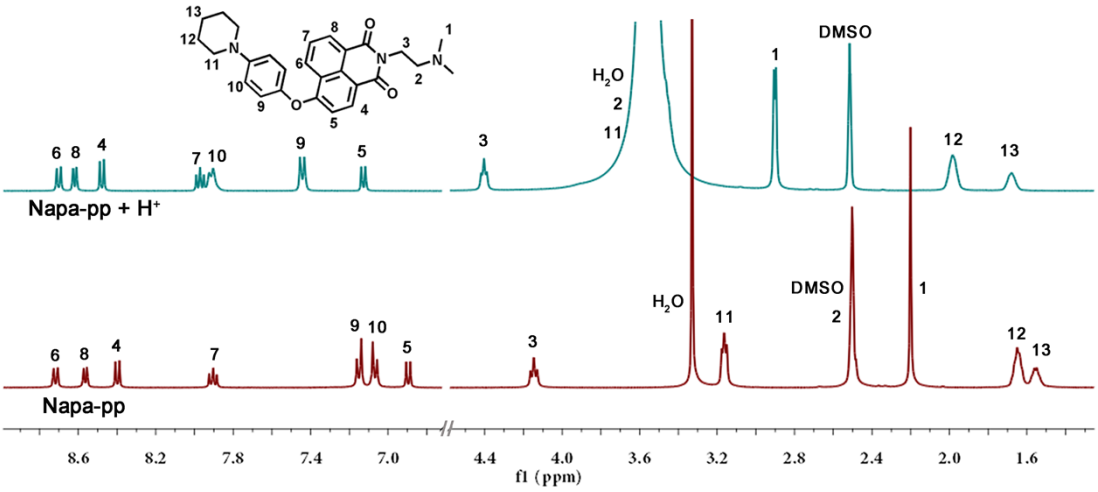

Figure S5 Partial ^{1}H NMR spectra of **Napa-pp** in DMSO-d_6 in the absence and presence of hydrochloric acid.

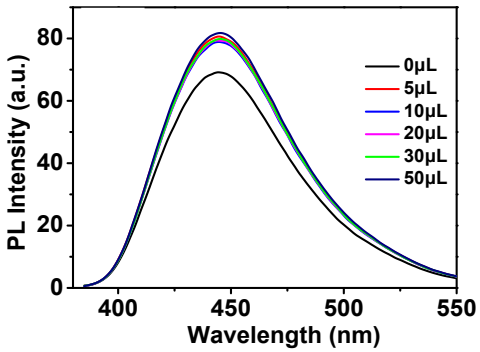

Figure S6 Fluorescence changes of **Napa-p** (15.8 μM in DMSO) upon addition of 0.2 M HCl.

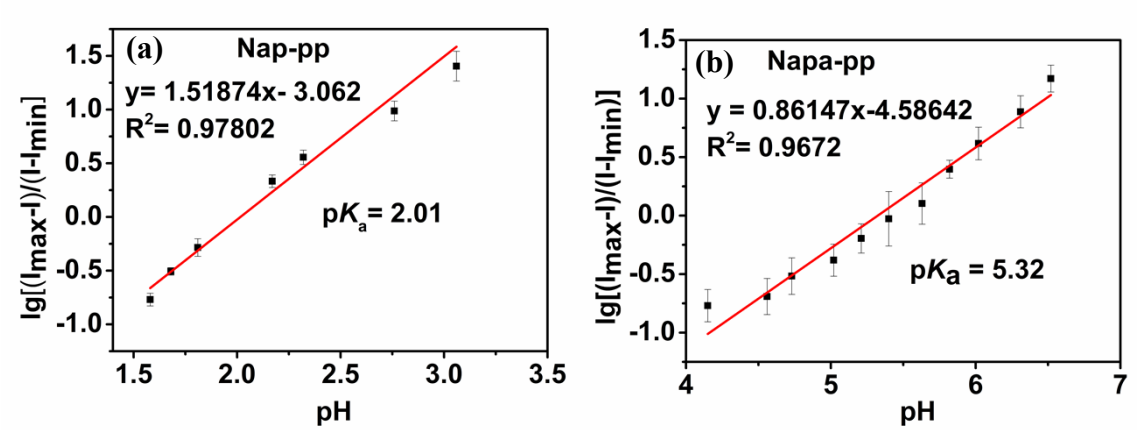

Figure S7 The fitted line of **Nap-pp** and **Napa-pp** toward variation on pH values in DMSO-H_2O buffer solution (1:250, v/v).

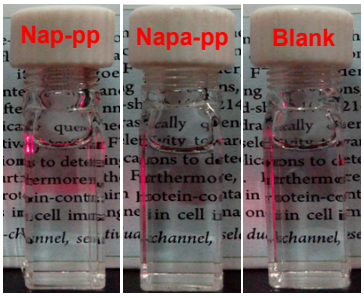

Figure S8 Light scattering experimental results of **Nap-pp**, **Napa-pp** and blank DMSO-PBS buffer solution (1:250, v/v, pH=7.0).

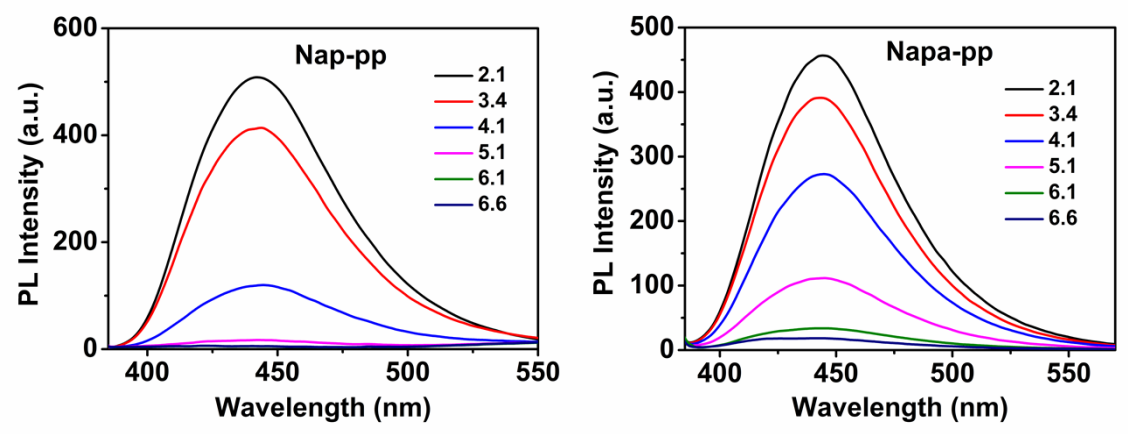

Figure S9 PL emission spectra of **Nap-pp** (5.3 μM) and **Napa-pp** (4.5 μM) toward variation on pH values in DMSO-H_2O buffer solution (1:1, v/v).

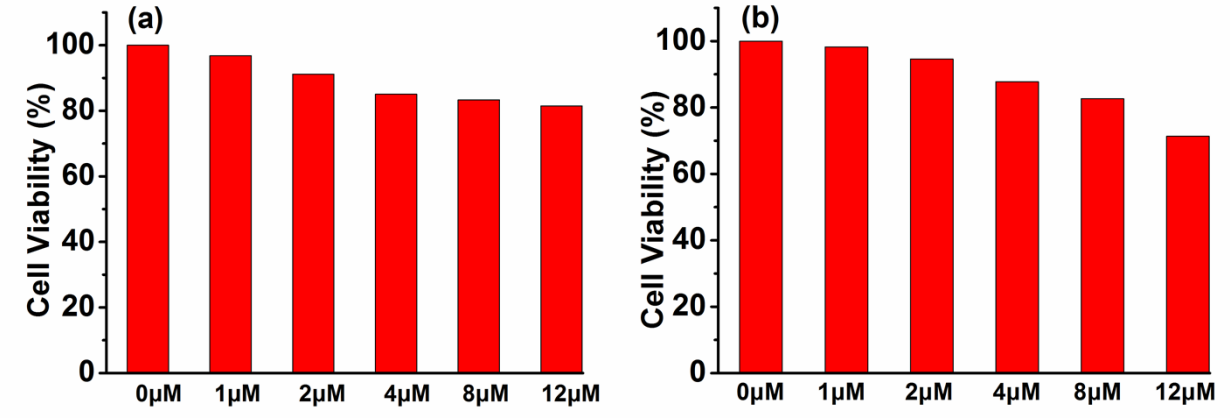

Figure S10 The cell viability of **Napa-pp** with different concentrations (0-12 μM) for (a) HeLa cells and (b) Raw cells.

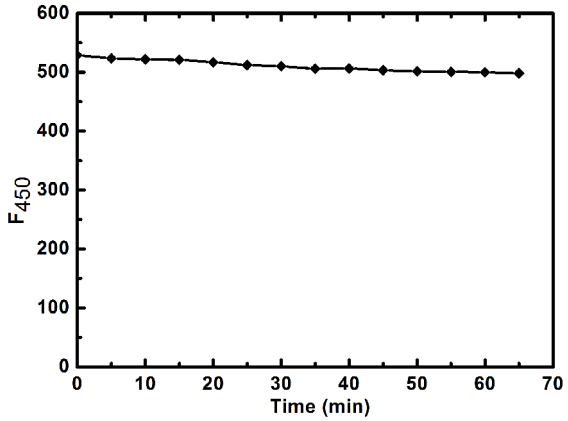

Figure S11 The time courses of PL intensity of **Napa-pp** (4.5 μM) in DMSO-H_2O buffer solution (1:250, v/v, pH = 5.0 λ_{em} = 450 nm).

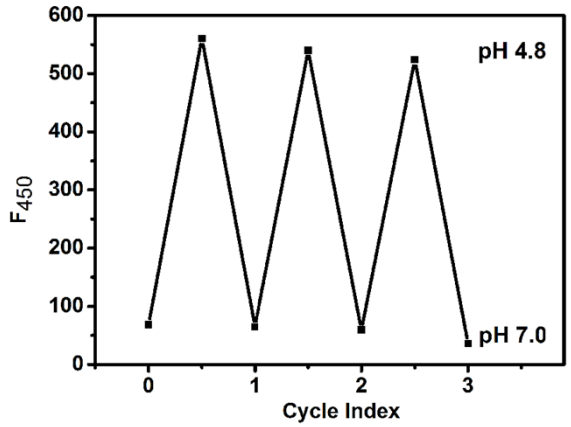

Figure S12 Reversible fluorescence changes of **Napa-pp** (4.5 μM) in DMSO-H_2O solution (1:250, v/v) between pH 4.8 and 7.0 (λ_{em} = 450 nm).

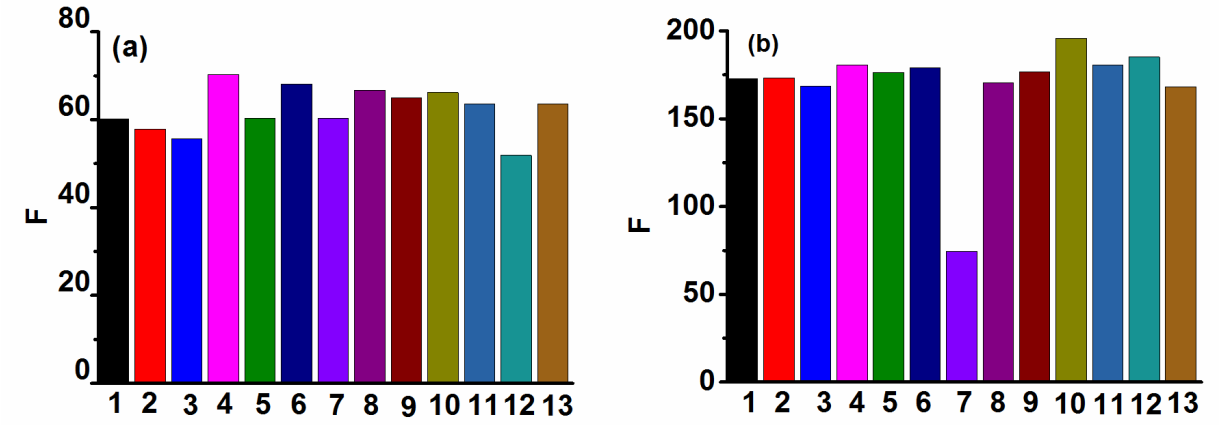

Figure S13 Emission spectra of **Napa-pp** (4.5 μM) in the presence of 13 μM various metal ions in buffer solutions of (a) pH =7.0, and (b) pH=5.0 : (1) blank, (2) Ba^{2+}, (3) Cr^{3+}, (4) Fe^{2+}, (5) Mn^{2+} , (6) Ni^{2+}, (7) Cu^{2+}, (8) Ca^{2+}, (9) Na^{+}, (10) K^{+}, (11) Zn^{2+}, (12) Fe^{3+}, (13) Mg^{2+}, λ_{em} = 450 nm.

2 Experimental details

1) General

All the chemicals commercially available were used directly without further purification unless otherwise stated. All the solvents were of analytical grade and freshly distilled prior to use. All the four objective compounds have been carefully purified via recrystallization for more than three times followed by vacuum sublimation to afford satisfactory purity. All the photophysical experiments were conducted under nitrogen atmosphere to exclude the interference of oxygen. All the photoluminescence characterizations were carried out at 298 K under excitation of 365 nm. ^{1}H NMR and ^{13}C NMR spectra were measured using a Bruker Avance AV II-400 MHz spectrometer, and the chemical shifts were recorded in units of ppm with TMS as the internal standard. Coupling constants (*J*) are reported in Hertz. High resolution MS spectra were measured with a Q-TOF Premier ESI mass spectrometer (Micromass, Manchester, UK). UV-Vis absorption spectra in solution were measured on a Perkin–Elmer Lambda 950 scanning spectrophotometer. PL spectra were recorded on a Perkin–Elmer LS55 fluorescence spectrophotometer at 298 K. PLQYs in dilute solution were determined using quinine sulfate in 0.05 mol·L^{-1} H_2SO_4 (φ = 0.55) as standard under excitation of 365 nm. The transient photoluminescence decay characteristics of the N_2 pre-degassed solution samples were recorded on a Single Photon Counting Controller FluoroHub-B. The pH values were controlled by PHS-3E meter calibrated at 298 K with standard buffers of pH 6.86 and 4.00. The buffers were adjusted to a constant ionic strength of 100 mM as the background electrolyte. Melting points were determined on a X-6 microscopic melting point apparatus. Room temperature referred to ambient temperature (25 °C). Heated experiments were conducted using thermostatically controlled oil baths. Reactions were monitored by thin layer chromatography (TLC) using silica 60 (F254) plates, visualized using 254 nm as appropriate excitation source. Silica column chromatography was carried out routinely using 40-60 Å silica gel. The metal ions, including Ba^{2+}, Cr^{3+}, Fe^{2+}, Mn^{2+} , Ni^{2+}, Cu^{2+}, Ca^{2+}, Na^{+}, K^{+}, Zn^{2+}, Fe^{3+}, Mg^{2+} were prepared in triple-distilled water. The buffer solutions with pH range of 3.5-5.4 were prepared by adjusting the HAc/NaAc composite system with pH values of 6.7 and 3.4; the buffer solutions with pH range of 0.9-3.3 were prepared by adjusting the H_3PO_4/NaH_2PO_4 composite system with pH values of 4.4 and 0.6; while the buffer solutions with pH range of 5.5-7.0 were prepared by adjusting the NaH_2PO_4/Na_2HPO_4 composite system with pH values of 7.2 and 5.6.

2) X-ray Crystallographic Analysis

Single crystal of compound **Napa-pp** suitable for X-ray diffraction analysis was obtained by slow crystallization in MeOH/DCM. The determination of the unit cell and data collection for the single crystal sample of **Napa-pp** was performed on a Xcalibur E X-ray single crystal diffractometer equipped with graphite monochromator Mo Kα (λ = 0.71073 Å) radiation. The data collection was executed using CrysAlisPro[1] program. Structure was solved by direct method and successive Fourier difference S 24 syntheses (SHELXS-97), and was refined by full-matrix least-squares procedure on F^2 with anisotropic thermal parameters for all non-hydrogen atoms (SHELXL-97).[2] Pictorial representations and measurements of twist angles of the crystal were outlined with Platon[3] and Mercury[4] program. The crystallographic data for **Napa-pp** had been deposited in the Cambridge Database (CCDC 990189).

3) Fluorescence Titrations and Calculation of pK_a Values

pK_a values of **Napa-pp** and **Nap-pp** were calculated by regression analysis of the fluorescence data to fit eq (1).[5] *F* is the emission intensity at a fixed wavelength 450 nm (λ_{ex} = 365 nm). F_{max} and F_{min} are the corresponding maximum and minimum limiting values of *F*, respectively.

$$pK_a = pH + \log \frac{F_{max} - F}{F - F_{min}} \qquad (1)$$

4) Quantum Chemical Calculations

Density functional theory (DFT) and time-dependent DFT (TD-DFT) at the B3LYP/6-31G (d) level were employed to investigate the optimized geometries and electronic structures of the ground state and the first excited states of **Napa-pp**, respectively. The structure of neutral **Napa-pp** was initially taken from the crystal structure (Figure S1) and further optimized. Vibrational frequency calculations for **Napa-pp** were carried out to make sure that the optimized structures were true energy minima. The solvation effects were modeled by applying the self-consistent reaction field (SCRF) under the polarizable continuum model (PCM) incorporating DCM as the solvent. All calculations were carried out using the Gaussian 09 program.[6]

5) Reversibility Response of Napa-pp Toward H^+ ion

To investigate the reversibility of the pH response of **Napa-pp**, the fluorescence intensity (at λ_{em} = 450 nm) of **Napa-pp** (4.5 μM) in PBS buffer solution with pH =7.0 was recorded first, then the solution was adjusted to pH 4.8 with aq. HCl solution (10 M), and the PL intensity was measured. After that, the solution was adjusted to pH 7.0 with aq. NaOH solution (8 M), and the PL intensity was recorded. The above processes were repeated for three times.

6) In vitro Bioimaging of HeLa Cells

HeLa cells were cultured in DMEM medium with 10% fetal bovine serum (Hyclone), 1% penicillin streptomycin combination (Hyclone), and incubated in a humidified atmosphere of 5% CO_2 at 37°C with the medium changed every other day. Cells were seeded in 35mm glass-bottom culture dishes at a density of 1×10^5 cells per dish. After 24h incubation, **Nap-pp** and **Napa-pp** were added into the medium at a concentration of 4 μM and then incubated for 0.5 h. The medium was removed and cells were washed 3 times with PBS, and added 500 μL fresh growth medium into each dish. And under confocal laser scanning microscopy (CLSM; TCS SP4, Leica Microsystems, Germany), these sensors were excited at 405 nm and their emission was collected from 425 nm to 500 nm, while lysotracker was excited at 543 nm and its emission was collected from 570-630 nm. Lysosome location experiment follows: Cells were seeded in 35 mm glass-bottom culture dishes at a density of 1×10^5 cells per dish. After 24 h incubation, the growth medium was removed and the fresh growth medium with 75 nM LysoTracker Red DND-99 (life technologies) were added into dishes for 0.5 h, followed by 4.0 μM **Napa-pp** for another 0.5 h in CO_2 incubator. After that, the medium was removed and the cells were washed with phosphate buffered saline (PBS) for 3 times. Then 1.5 mL PBS was added into dishes.

7) Synthetic Procedures and Characterization Data of the Intermediates and Objective Compounds

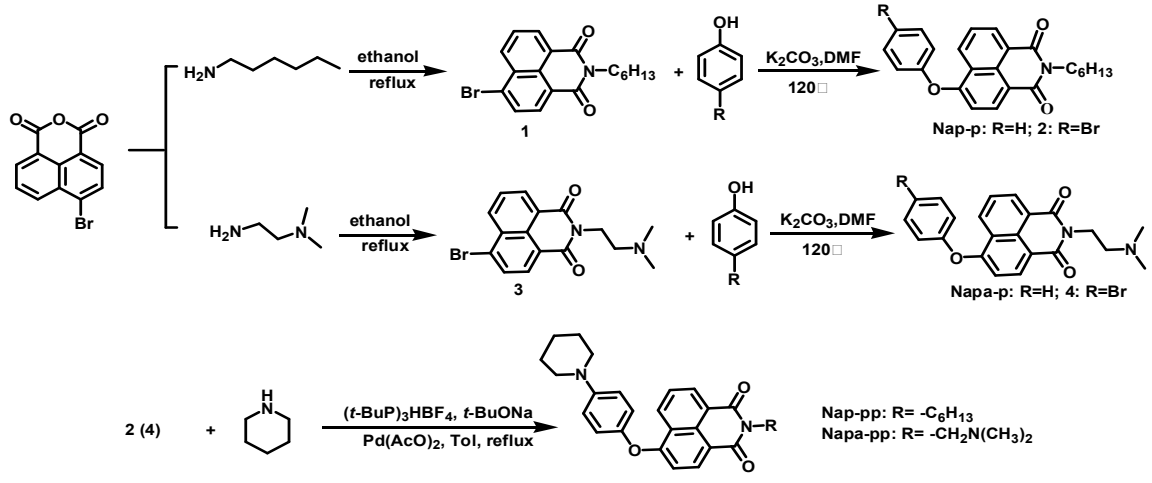

Scheme S1 Synthetic routes toward the four compounds investigated in this article

6-Bromo-2-hexyl-1*H*-benzo[*de*]isoquinoline-1,3(2*H*)-dione (1)[7]: 4-Bromo-1,8-naphthalic anhydride (4.00 g, 14.4 mmol) and 1-hexanamine (1.62 g, 16 mmol) were stirred in ethanol solution (54 mL) under 80 °C for 12 h. The reactant mixture was filtered to remove excessive 1-hexanamine and the collected precipitate was crystallized from acetone/ethanol to obtain white solid. Yield: 75%. Melting point: 180-181 °C.

6-(4-Bromophenoxy)-2-hexyl-1*H*-benzo[*de*]isoquinoline-1,3(2*H*)-dione (2)[8]: To a solution of **1** (1.04 g，2.9 mmol) in anhydrous DMF (10 mL) was added potassium carbonate (1.59 g，11.5 mmol) and 4-bromo-phenol (1.04 g，6 mmol). Then the mixture was allowed to stir for 2.5 h at 120 °C under N_2. After cooled down, the mixture was poured into water and the white solid was collected, washed with water and dried in vacuo. The crude product was purified by column chromatography (eluent: petroleum ether/ DCM = 1/1, v/v), Pale yellow powder, recrystallized from ethanol. Yield: 73%, melting point: 149-150 °C. ^{1}H NMR ($CDCl_3$, 400 MHz) δ 8.71-8.64 (m, 2H, NapH), 8.48 (d, 1H, *J* = 8.4 Hz, NapH), 7.81-7.77 (m, 1H, ArylH), 7.61-7.57 (m, 2H, ArylH), 7.10-7.07 (m, 2H, ArylH), 6.94 (d, 1H, *J* = 8.0 Hz, NapH), 4.17 (t, 2H, *J* = 7.6 Hz, -CH_2), 1.76-1.69 (m, 2H, -CH_2), 1.46 - 1.28 (m, 6H, -CH_2), 0.89 (t, 3H, *J* = 6.8 Hz, -CH_3).

6-Bromo-2-(2-(dimethylamino)ethyl)-1*H*-benzo[*de*]isoquinoline-1,3(2*H*)-dione (3)[9]: The synthetic method for substrate **3** was similar to the synthesis of substrate **1**. Yellow powder, recrystallized from ethanol. Yield: 85.3%, melting point: 148-149 °C. ^{1}H NMR (400 MHz, $CDCl_3$) δ 8.65 (d, *J* = 8.0 Hz, 1H, NapH), 8.56 (d, *J* = 8.0 Hz, 1H, NapH), 8.41 (d, *J* = 8.0 Hz, 1H, NapH), 8.03 (d, *J* = 8.0 Hz, 1H, NapH), 7.84 (t, *J* = 8.0 Hz, 1H, NapH), 4.32 (t, *J* = 8.0 Hz, 2H, -CH_2), 2.65 (t, *J* = 8.0 Hz, 2H, -CH_2), 1.65 (s, 6H, -CH_3).

6-(4-Bromophenoxy)-2-(2-(dimethylamino)ethyl)-1*H*-benzo[*de*]isoquinoline-1,3(2*H*)-dione (4): The synthetic method for substrate **4** was similar to the synthesis of substrate **2**. White solid powder, recrystallized for four times from ethanol. Yeild: 72%, melting point: 168-169 °C. ^{1}H NMR ($CDCl_3$, 400 MHz) δ 8.68 (d, 2H, *J* = 8.0 Hz, NapH), 8.48 (d, 1H, *J* = 8.0 Hz, NapH), 7.79 (t, 1H, *J* = 8.0 Hz, NapH), 7.61 (mm, 2H, ArylH), 7.10 (mm, 2H, ArylH), 6.93 (d, 1H, *J* = 8.0 Hz, NapH), 4.42 (t, 2H, J = 8.0 Hz, -CH_2), 2.91 (s, 2H, -CH_2), 2.56 (s, 6H, -CH_3).

2-Hexyl-6-phenoxy-1*H*-benzo[*de*]isoquinoline-1,3(2*H*)-dione (Nap-p)[8]: The crude product was purified by column chromatography (eluent: petroleum ether/ DCM = 1/1, v/v), followed by recrystallizing for four times from ethanol to afford white needles crystal with yield of 82%. Melting point: 86-87 °C. ^{1}H NMR ($CDCl_3$, 400 MHz) δ 8.72 (dd, *J* = 8.4 Hz , *J* = 0.8 Hz, 1H, NapH), 8.67 (dd, *J* = 7.6 Hz, *J* = 0.8 Hz,1H, NapH), 8.47 (d, *J* = 8.4 Hz, 1H, NapH), 7.80 (t, *J* = 8.0 Hz, 1H, NapH), 7.51 (t, *J* = 8.0 Hz ,2H, ArylH), 7.47-7.29 (m, 1H, ArylH), 7.20 (dd, *J* = 8.4 Hz, J = 0.8 Hz, 2H, ArylH), 6.92 (d, *J* = 8.4 Hz, 1H, NapH), 4.19 (t, *J* = 7.6 Hz, 2H, -CH_2), 1.75-1.71 (m, 2H, -CH_2), 1.45-1.41 (m, 2H, -CH_2), 1.36-1.32 (m, 4H, -CH_2), 0.91 (t, *J* = 6.8 Hz, 3H, -CH_3). ^{13}C NMR ($CDCl_3$, 100 MHz) δ 164.4 (1C, -C=O, Nap), 163.7 (1C, -C=O, Nap), 159.8 (1C, Nap), 154.8 (1C, -C-O, Aryl), 132.7 (1C,

Nap), 131.8 (1C, Aryl), 130.4 (2C, Aryl), 129.7 (1C, Nap), 128.5 (1C, Nap), 126.5 (1C, Nap), 125.6 (1C, Nap), 123.9 (1C, Nap), 122.7 (1C, Nap), 120.8 (2C, Aryl), 116.6 (1C, Nap), 110.6 (1C, Nap), 77.3 (1C, -CH_2), 77.2 (1C, -CH_2), 77.0 (1C, -CH_2), 76.7 (1C, -CH_2), 40.4 (1C, -CH_2), 31.6 (1C, -CH_2), 28.1 (1C, -CH_2), 26.8 (1C, -CH_2), 22.6 (1C, -CH_2), 14.1 (1C, -CH_3). HRMS (ESI^+) m/z calculated for $C_{24}H_{24}NO_3$ $(M+H)^+$: 371.1756, found 374.1757.

6-(4-Phenoxy)-2-(2-(dimethylamino)ethyl)-1*H*-benzo[*de*]isoquinoline-1,3(2*H*)-dione (Napa-p): Recrystallized for four times from ethanol to afford white solid powder. Yeild: 75%, melting point: 146-147 °C. ^{1}H NMR ($CDCl_3$, 400 MHz) 8.72 (dd, 1H, *J* = 8.4 Hz, *J* = 1.2 Hz, NapH), 8.67 (dd, 1H, *J* = 7.2 Hz, *J* = 1.2 Hz, NapH), 8.47 (d, 1H, *J* = 8.4 Hz, NapH), 7.78 (t, 1H, *J* = 8 Hz, NapH), 7.49 (t, 2H, *J* = 7.6 Hz, ArylH), 7.31 (t, 1H, *J* = 7.2 Hz, ArylH), 7.21 (dd, 2H, *J* = 8.4 Hz, *J* = 0.8 Hz, ArylH), 6.92 (d, 1H, *J* = 8 Hz, NapH), 4.34 (t, 2H, *J* = 7.2 Hz, -CH_2), 2.67 (t, 2H, *J* = 7.2 Hz, -CH_2), 2.38 (s, 6H, -CH_3). ^{13}C NMR ($CDCl_3$, 100 MHz) δ 164.4 (1C, -C=O, Nap), 163.8 (1C, -C=O, Nap), 159.9 (1C, Nap), 154.8 (1C, -C-O, Aryl), 132.9 (1C, Nap), 132.0 (1C, Aryl), 130.4 (2C, Aryl), 129.7 (1C, Nap), 128.6 (1C, Nap), 126.5 (1C, Nap), 125.6 (1C, Nap), 123.9 (1C, Nap), 122.6 (1C, Nap), 120.8 (2C, Aryl), 116.5 (1C, Nap), 110.6 (1C, Nap), 57.0 (1C, -CH_2), 45.8 (2C, -$N(CH_3)_2$), 38.1 (1C, -CH_2). HRMS (ESI^+) m/z calculated for $C_{22}H_{21}N_2O_3$ $(M+H)^+$: 361.1552, found 361.1558.

6-(4-Pieperidinylphenoxy)-2-hexyl-1*H*-benzo[*de*]isoquinoline-1,3(2*H*)-dione (Nap-pp): To a solution of **2** (1.8 g, 4 mmol) in anhydrous toluene (50 mL) were added (t-Bu)$_3$PHBF_4 (48.6 mg, 0.17 mmol), *t*- BuONa (2.31 g, 24 mmol), $Pa(AcO)_2$ (26.94 mg, 0.12 mmol) and piperidines (0.75 g, 8.8 mmol). Then the mixture was refluxed for 8 h at 120 °C under N_2. The system was filtered and concentrated in vacuum. The crude product was purified by column chromatography (eluent: petroleum ether/ DCM = 1/1, v/v and recrystallized for five times from ethanol to render orange-yellow plate crystal. Yield: 16%, melting point: 106-107 °C. ^{1}H NMR ($CDCl_3$, 400 MHz) 8.74 (dd, 1H, *J* = 8.4 Hz, *J* = 0.8 Hz, NapH), 8.66 (dd, 1H, *J* = 7.2 Hz, *J* = 1.2 Hz, NapH), 8.44 (d, 1H, *J* = 8.4 Hz, NapH), 7.77 (t, 1H, *J* = 7.8 Hz, NapH), 7.09 (d, 2H, *J* = 9.2 Hz, ArylH), 7.04 (d, 2H, *J* = 8.8 Hz, ArylH), 6.87 (d, 1H, *J* = 8.4 Hz, NapH), 4.16 (t, 2H, *J* = 7.6 Hz, -CH_2), 3.19 (t, 4H, *J* = 5.2 Hz, -CH_2 (piperidinyl)), 1.76-1.69 (m, 6H, -CH_2 and -CH_2 (piperidinyl)), 1.64-1.59(m, 2H, -CH_2 (piperidinyl)), 1.46-1.39 (m, 2H, -CH_2), 1.35-1.32 (m, 4H，-CH_2), 0.89 (t, 3H, *J* = 6.8 Hz, -CH_3). ^{13}C NMR ($CDCl_3$, 100 MHz) δ 164.6 (1C, -C=O, Nap), 164.0 (1C, -C=O, Nap), 161.0 (1C, -C-O, Nap), 150.3 (1C, Nap), 146.9 (1C, -C-O, Aryl), 133.0 (1C, Aryl), 131.9 (1C, Nap), 129.7 (1C, Nap), 128.7 (1C, Nap), 126.3 (1C, Nap), 123.7 (1C, Nap), 122.7 (1C, Nap), 121.7 (2C, Aryl), 118.1 (2C, Aryl), 116.0 (1C, Nap), 109.7 (1C, Nap), 51.1 (2C, piperidinyl), 40.5 (1C, -CH_2), 31.7 (1C, -CH_2), 29.8 (1C, -CH_2), 28.2 (1C, -CH_2), 26.9 (1C, -CH_2), 26.0 (2C, piperidinyl), 24.3 (1C, piperidinyl), 22.7 (1C, -CH_2), 14.2 (1C, -CH_3). HRMS (ESI^+) m/z calculated for $C_{29}H_{33}N_2O_3$ $(M+H)^+$: 457.2491, found 457.2490.

6-(4-Piperidinylphenoxy)-2-(2-(dimethylamino)ethyl)-1*H*-benzo[*de*]isoquinoline-1,3(2*H*)-dione (Napa-pp): The synthetic method for substrate **Napa-pp** was similar to the synthesis of substrate **Nap-pp**. The crude product was purified by column chromatography (eluent: DCM/ MeOH = 25/1, v/v) and recrystallized for five times from ethanol to render yellow plate crystal. Yield: 15%, melting point: 156-157 °C. ^{1}H NMR ($CDCl_3$, 400 MHz) 8.74 (dd, 1H, *J* = 8 Hz, *J* = 0.8 Hz, NapH), 8.66 (dd, 1H, *J* = 7.2

Hz, J = 0.8 Hz, NapH), 8.44 (d, 1H, J = 8 Hz, NapH), 7.77 (t, 1H, J = 8 Hz, NapH), 7.10-7.06 (m, 2H, ArylH), 7.04 - 7.00 (m, 2H, ArylH) , 6.86 (d, 1H, J = 8.4 Hz，NapH) , 4.33 (t, 2H, J = 6.8 Hz, -CH_2), 3.19 (t, 4H, J = 5.2 Hz, -CH_2 (piperidinyl)), 2.65 (t, 2H, J = 7.2 Hz, -CH_2), 2.36 (s, 6H, -CH_3), 1.78 - 1.73 (m, 4H, -CH_2 (piperidinyl)), 1.64 - 1.58 (m, 2H, -CH_2 (piperidinyl)). ^{13}C NMR ($CDCl_3$, 100 MHz) δ 164.6 (1C, -C=O, Nap), 164.0 (1C, -C=O, Nap), 161.1(1C, -C-O, Nap), 150.4 (1C, Nap), 146.8 (1C, -C-O, Aryl), 133.2 (1C, Aryl), 132.0 (1C, Nap), 129.8 (1C, Nap), 128.9 (1C, Nap), 126.3 (1C, Nap), 123.7 (1C, Nap), 122.6 (1C, Nap), 121.7 (2C, Aryl), 118.1 (2C, Aryl), 115.9 (1C, Nap), 109.6 (1C, Nap), 57.1 (1C, -CH_2), 51.1 (2C, -$N(CH_3)_2$), 45.9 (2C, piperidinyl), 38.1 (1C, -CH_2), 26.0 (2C, piperidinyl), 24.3(1C, piperidinyl). HRMS (ESI^+) m/z calculated for $C_{27}H_{30}N_3O_3$ $(M+H)^+$: 444.2287, found 444.2284.

Reference

(1) Oxford Diffraction, CrysAlisPro CCD and CrysAlisPro RED, including ABSPACK. Oxford, Diffraction Ltd., Yarnton, England, 2009.

(2) Sheldrick, G. M. SHELXS-97, Program for Refinement of Crystal Structure. University of Gottingen, Gottingen, Germany, 1997.

(3) A. L. Spek, *J. Appl. Crystallogr.,* 2003, **36**, 7.

(4) I. J. Bruno, J. C. Cole, P. R. Edgington, M. K. Kessler, C. F. Macrae, P. McCabe, J. Pearson and R. Taylor, *Acta Crystallogr. Sect. B: Struct. Sci.,* 2002, **B58**, 389.

(5) (a) W. W. Qin, M. Baruah, A. Stefan, M. Auweraer Van der, and N. Boens, *Chem. Phys. Chem.,* 2005, **6**, 2343. (b) E. Cielen, A. Tahri, A. Ver Heyen, G. J. Hoornaert, F. C. De Schryver, N. Boens, *J. Chem. Soc., Perkin Trans.*, 1998, **2**, 1573. (c) M. Baruah, W. W. Qin, N. Basaric´, W. M. De Borggraeve, and N. Boens, *J. Org. Chem*., 2005, **70**, 4152.

(6) Gaussian 09, Revision B.01: Frisch, M. J.; Trucks, G. W.;Schlegel, H. B.; Scuseria, G. E.; Robb, M. A.; Cheeseman, J. R.;Montgomery, J. A., Jr.; Vreven, T.; Kudin, K. N.; Burant, J. C.; Millam,J. M.; Iyengar, S. S.; Tomasi, J.; Barone, V.; Mennucci, B.; Cossi, M.;Scalmani, G.; Rega, N.; Petersson, G. A.; Nakatsuji, H.; Hada, M.;Ehara, M.; Toyota, K.; Fukuda, R.; Hasegawa, J.; Ishida, M.;Nakajima, T.; Honda, Y.; Kitao, O.; Nakai, H.; Klene, M.; Li, X.;Knox, J. E.; Hratchian, H. P.; Cross, J. B.; Adamo, C.; Jaramillo, J.;Gomperts, R.; Stratmann, R. E.; Yazyev, O.; Austin, A. J.; Cammi, R.;Pomelli, C.; Ochterski, J. W.; Ayala, P. Y.; Morokuma, K.; Voth, G. A.;Salvador, P.; Dannenberg, J. J.; Zakrzewski, V. G.; Dapprich, S.;Daniels, A. D.; Strain, M. C.; Farkas, O.; Malick, D. K.; Rabuck,A. D.; Raghavachari, K.; Foresman, J. B.; Ortiz, J. V.; Cui, Q.; Baboul,A. G.; Clifford, S.; Cioslowski, J.; Stefanov, B. B.; Liu, G.; Liashenko,A.; Piskorz, P.; Komaromi, I.; Martin, R. L.; Fox, D. J.; Keith, T.; M. A. Al-Laham, Peng, C. Y.; Nanayakkara, A.; Challacombe, M.; Gill,P. M. W.; Johnson, B.; Chen, W.; Wong, M. W.; Gonzalez, C.; Pople,J. A. Gaussian, Inc., Pittsburgh, PA, 2009.

(7) Y. Nagao, T. Yoshida and K. Arimitsu, *Heterocycles,* 2010, **80**, 1197.

(8) J. L. Magalhaes, R. V. Pereira, E. R. Triboni, F. P. Berci, M. H. Gehlen and F. C. Nart, *J. Photochem. Photobiol. A: Chem.,* 2006, **183**, 165.

(9) H. H. Lin, Y. C. Chan, J. W. Chen and C. C. Chang, *J. Mater. Chem.,* 2011, **21**, 3170.

3. ^{1}H NMR and ^{13}C NMR spectra of the objective compounds

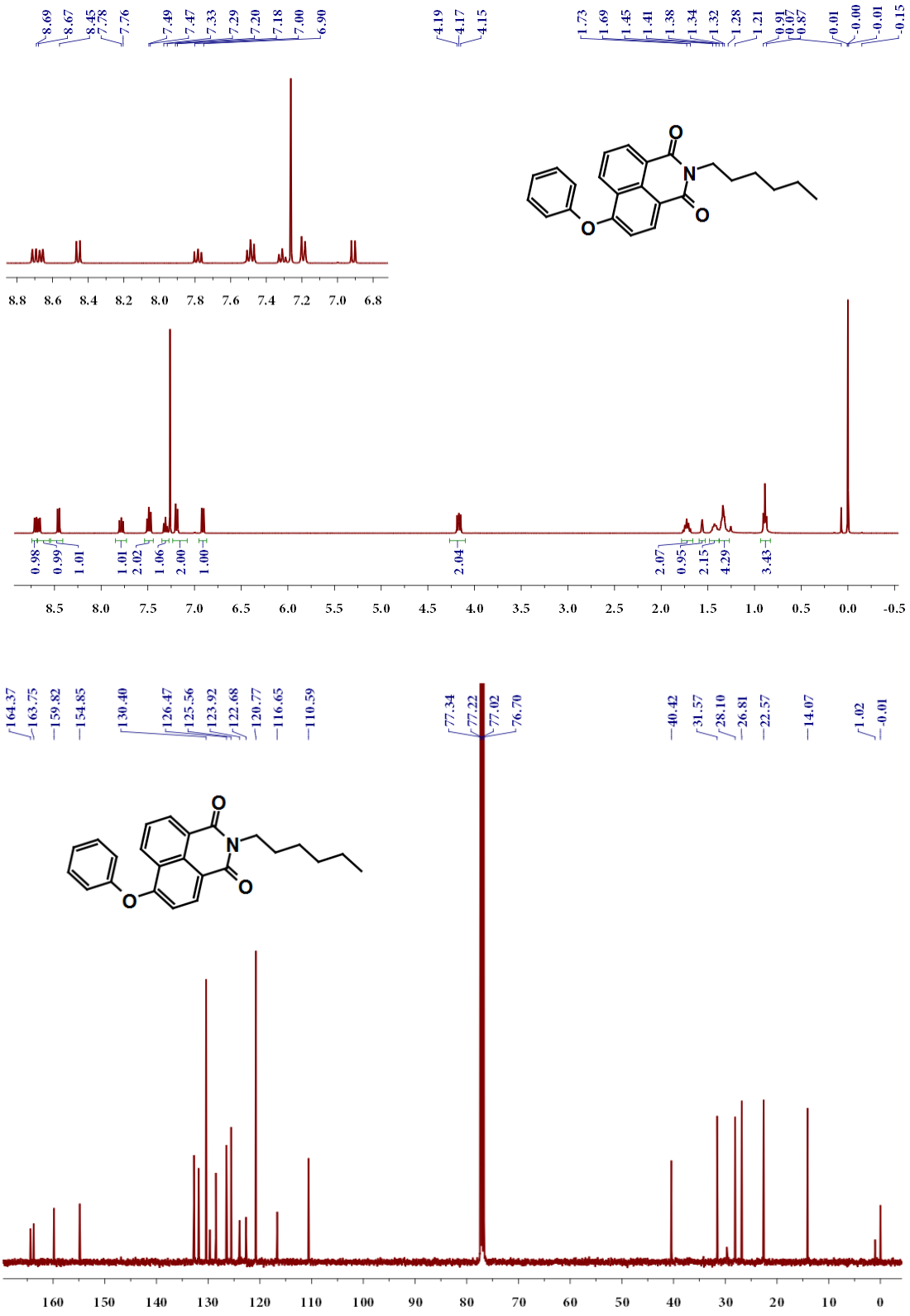

^{1}H NMR and ^{13}C NMR spectra of **Nap-p**.

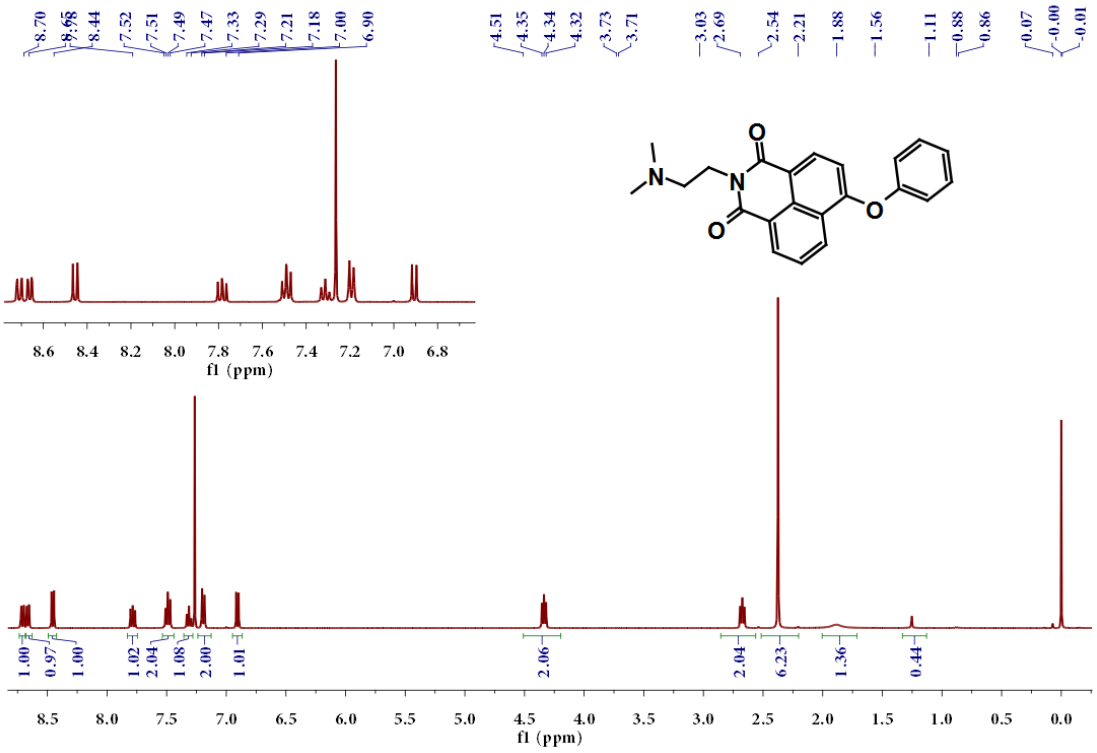

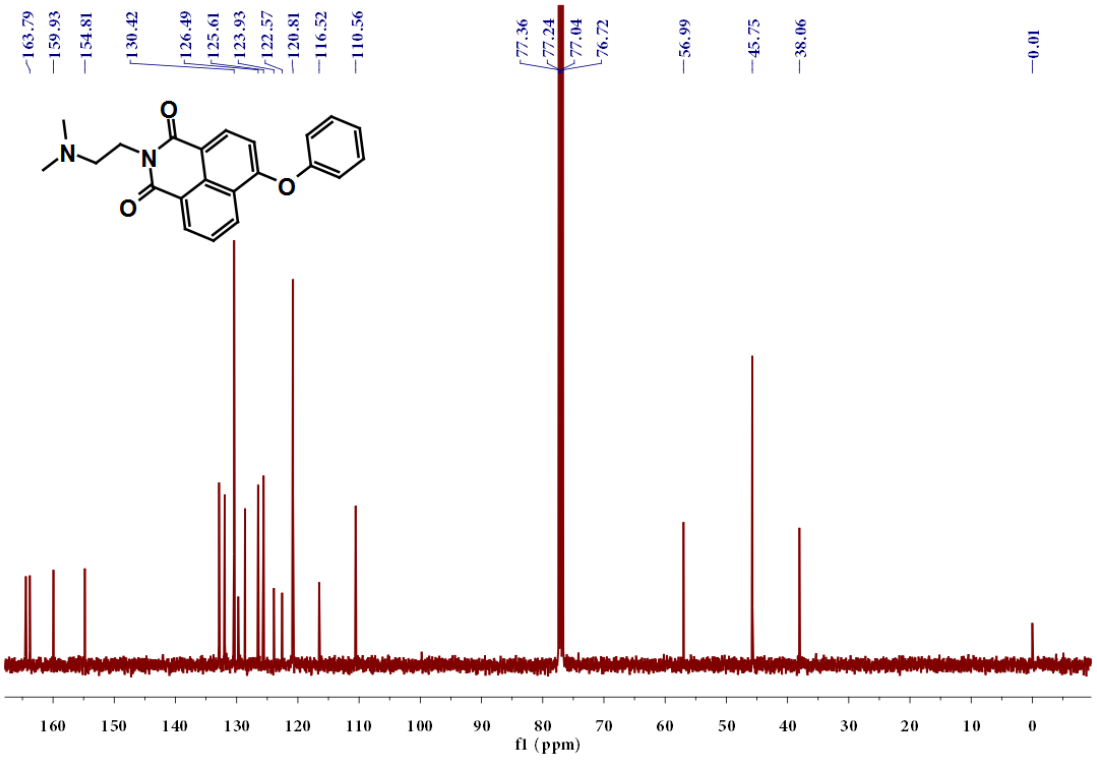

^{1}H NMR and ^{13}C NMR spectra of **Napa-p**.

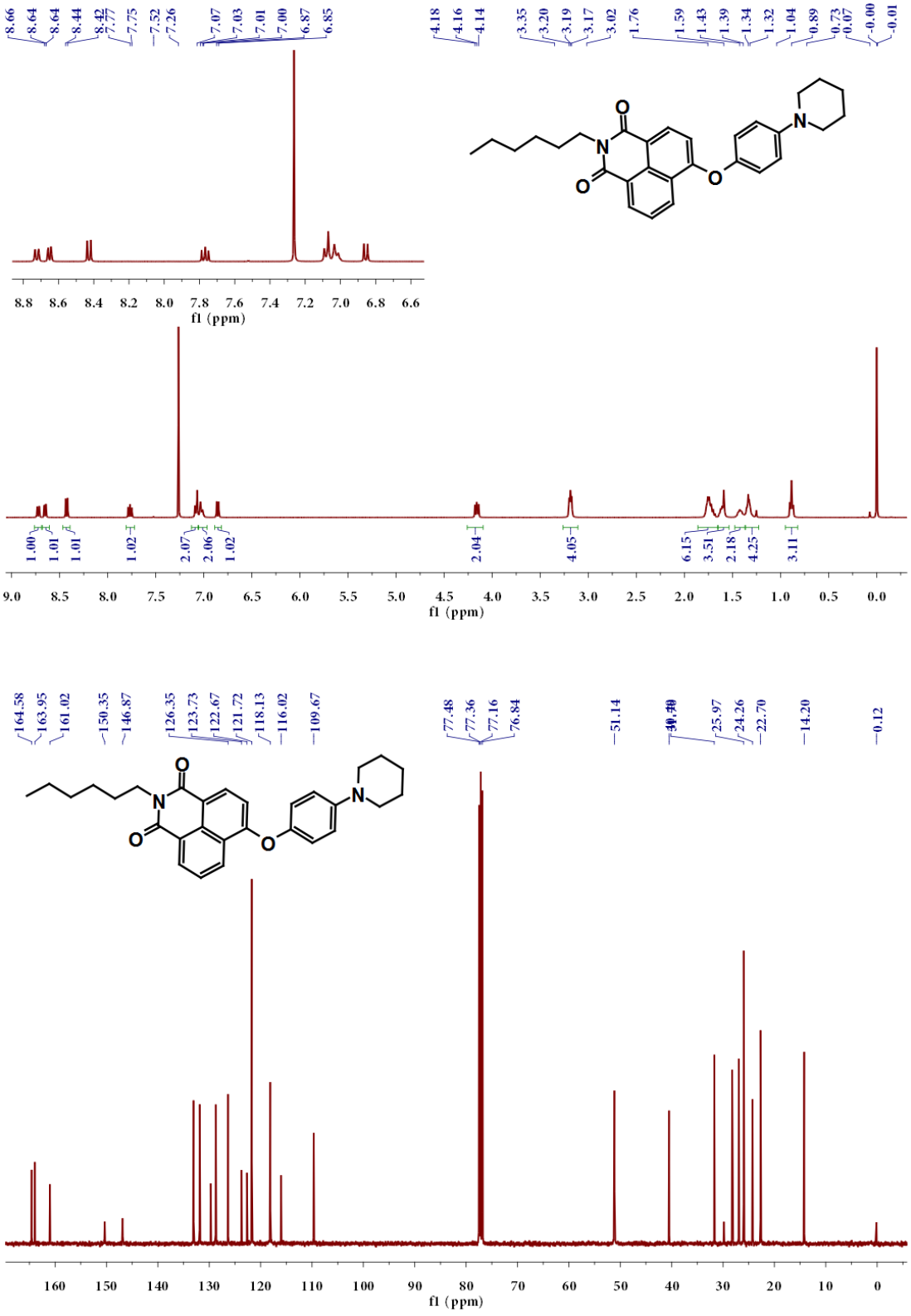

^{1}H NMR and ^{13}C NMR spectra of **Nap-pp**.

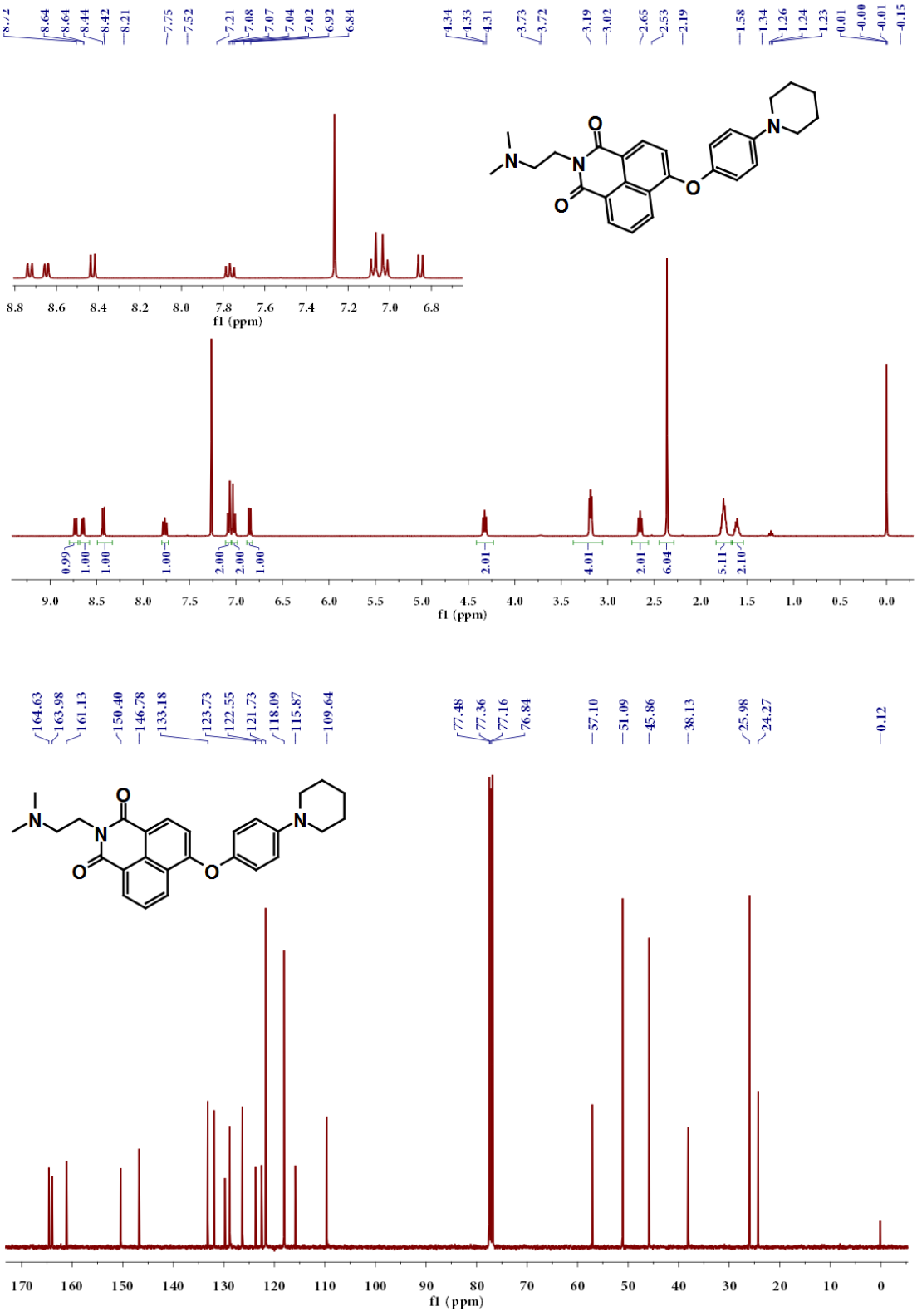

^{1}H NMR and ^{13}C NMR spectra of **Napa-pp**.

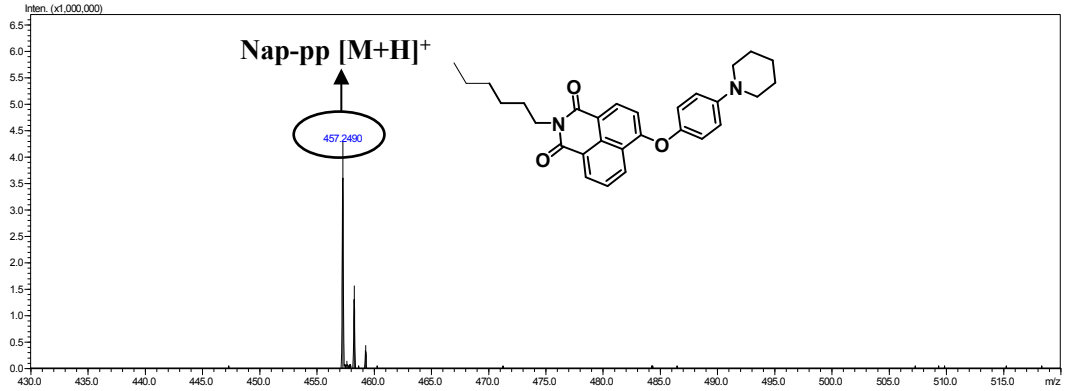
Inten. (x1,000,000)
Nap-pp [M+H]+
457.2490
O
N
O
O
N
m/z

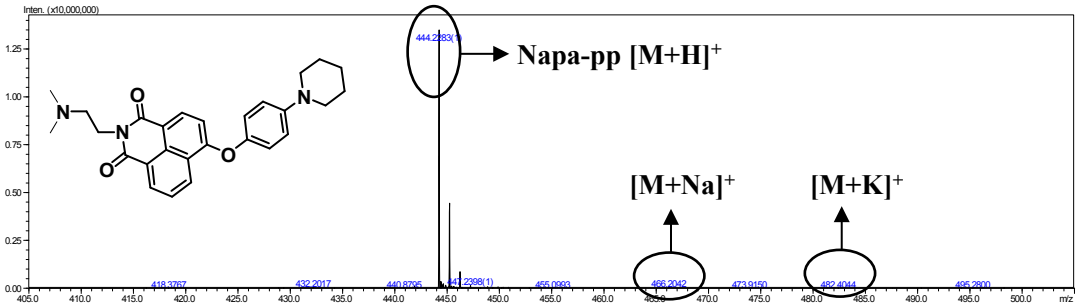
Inten. (x10,000,000)
444.2283(1)
Napa-pp [M+H]+
[M+Na]+
[M+K]+
418.3767
432.2017
440.0795
442.2398(1)
455.0993
466.2042
473.9150
482.4044
495.2800
m/z